

## Optically Active Polyethers. 2. Atomic Force Microscopy of Melt-Crystallized Poly(epichlorohydrin) Enantiomers and Their Equimolar Blend

K. L. Singfield, J. M. Klass, and G. R. Brown\*

Department of Chemistry, McGill University, 801 Sherbrooke Street West, Montreal, Quebec, Canada, H3A 2K6

Received May 31, 1995; Revised Manuscript Received August 17, 1995\*

**ABSTRACT:** The surface morphologies of melt-crystallized spherulites of the optically active *R* and *S* forms of poly(epichlorohydrin) and their equimolar blend have been investigated by atomic force microscopy (AFM). For the banded spherulites formed from the optically pure polyenantiomers, a regular pattern of alternating concentric ridges and valleys observed by AFM corresponds directly to the pattern of birefringent extinction bands observed under the polarized light microscope. Examination of the surface topography of these banded spherulites, either by reflectance optical microscopy or by AFM, reveals a spiral form with a "sense" or handedness that is dependent on the chirality of the constituent polyenantiomer. In contrast, a relatively featureless surface is observed for the spherulites formed upon crystallization of the equimolar blend. AFM images of the spherulitic surface indicate the presence of predominantly flat lamellae in the equimolar blend while those of the pure polyenantiomer appear to have an alternating flat to edge-on orientation, corresponding to the banding pattern. These observations are discussed in the context of the current theories of lamellar organization in banded spherulites.

### Introduction

It is well known that chain-folded lamellae are the building blocks of melt-crystallized polymers. However, the detailed description of the geometry of individual lamellae and their organization in the multilayered crystal aggregates that form spherulites remains the subject of intense study. Traditionally, efforts to describe the fundamental features of lamellar organization in melt-crystallized polymers have been focused on polymers with a minimum degree of complexity, principally, polyethylene.<sup>1-12</sup> Consequently, the models that have been developed rely heavily on these rather ideal systems.

Detailed investigations have also been made of the morphology of isotactic polypropylene (i-PP), which is a more complex crystalline polymer owing to the pseudochiral nature of the chains.<sup>13-19</sup> The  $\alpha$ -monoclinic crystal form of i-PP is among the most thoroughly studied and hence best understood polymer crystalline forms. Chiral selection of the pseudochiral helices leads to the most stable phase of this crystalline form, in which there exist regularly alternating layers of right- and left-handed helices.

The extent to which the effects of *true* asymmetric centers along the polymer backbone can be transmitted to higher order structures has received limited attention<sup>20</sup> and invites further investigation. Macromolecular backbone chirality can impose characteristic secondary structures and, in turn, influence the mode of packing upon crystallization. Specifically, it can be envisioned that the effect of backbone chirality on the organization of molecular helices in the lamellae and, hence, the arrangement of neighboring lamellae, would be manifested in the overall morphology of the crystalline structure (e.g., a spherulite). In this way, the examination of the morphology of the spherulites of these optically active polymers could provide new insights into the organization of the lamellae within

spherulites. To the best of our knowledge, however, there are no reported studies which employ optical activity as an analytical tool for the elucidation of the spherulitic architecture of melt-crystallized synthetic polymers.

Poly(epichlorohydrin) is a polymer with chiral centers along its polyether backbone. Recently, we reported<sup>21</sup> that on crystallization from the melt, the optically pure polymer forms spherulites which, when examined by polarized light optical microscopy, exhibit a periodic pattern of birefringent extinction bands while the corresponding equimolar blend of the polyenantiomers forms nonbanded spherulites. An analysis of the observed differences in the crystallization kinetics and the morphology between the optically pure polyenantiomers and their blends led to the suggestion that in the blend a stereoselective mechanism operates at the growth front during isothermal crystallization.

The appearance of periodic birefringent extinction bands under transmitted polarized light is a relatively common feature in spherulites of crystalline polymers. It is well established that it is a regularly twisted molecular orientation about the radial growth axis that gives rise to this pattern.<sup>3-4,22-24</sup> However, a twisted molecular arrangement can be accommodated in more than one type of lamellar structure. The precise description of the shape and organization of the lamellae in these banded spherulites remains a subject of ongoing debate. Polyethylene,<sup>7-9</sup> a substituted polyethylene, poly(4-methyl-1-pentene),<sup>25</sup> and the more complex poly(vinylidene fluoride)<sup>26</sup> are among the few systems in which the geometry and the mutual dispositions of lamellae in banded spherulites have been examined in detail.

There currently exist two models which describe the form and organization of the lamellae within banded spherulites: (1) A twisted molecular geometry can be expressed at the lamellar level through a sequence of transverse screw dislocations of the same sign. Under isothermal crystallization conditions these are equally spaced along the radial growth direction of the lamella. Each screw dislocation supplies an increment of the

\* To whom correspondence should be addressed.

† Abstract published in *Advance ACS Abstracts*, October 15, 1995.

overall twist to the radially growing lamellae. The sense of the isochiral transverse dislocations is controlled by the direction of inclination of the chain stems with respect to the lamellar normal and the nature of the folding at the surface of an individual lamella. According to this model, the overall effect of neighboring, in-phase, dislocating lamellae gives rise to the observed banding pattern. This model, originally put forth by Schultz and Kinloch,<sup>27</sup> has since been modified and developed extensively by Bassett and co-workers.<sup>6-8,28</sup> Currently, the model holds that the chirality, or sense, of the dislocations is linked to the direction of tilt of the chain stems and is not associated with any stresses at the lamellar fold surfaces. At the screw dislocations, which serve as branch points in the spherulite, the adjacent lamellae which constitute the layers of the screw dislocation mutually diverge, enhancing the element of twist. This diversion is attributed to the pressure, between layers, due to uncrystallized molecular cilia associated with the fold surfaces of neighboring lamellae; i.e., there is an interlamellar origin to the lamellar geometry.

(2) A regularly twisted molecular orientation can also be accommodated in a continuously twisted helicoidal lamella without screw dislocations, as originally proposed by Keller.<sup>29</sup> The twisting is attributed mainly to the influence of the surface stresses arising from the disordered chain folds.<sup>30</sup> This model has been developed significantly by Keith and Padden.<sup>9</sup> The fold staggering causes the chain stems to be nonorthogonal to the fold surfaces. The nonorthogonal relationship between the lamellar faces and the chain axes creates unequal stresses at opposite fold surfaces. This, in turn, gives rise to bending moments and ultimately results in the twisting of the lamella. Screw dislocations may form in given regions as a consequence of contacts between growing, but already twisted, lamellae. The feature which determines the direction of twist, the so-called "chiral factor", is the direction of chain tilt with respect to the lamellar normal. Keith and Padden have thus focused on an intralamellar origin to the lamellar geometry.

Direct observation of melt-crystallized lamellae has routinely been achieved by electron microscopy. The application of transmission electron microscopy techniques is limited to very thin sections or films and, to a certain extent, tends to suffer from the inherent effects of sample irradiation. Developments in chemical etching,<sup>31</sup> decorating,<sup>32</sup> and staining<sup>33</sup> as sample preparation techniques have helped to minimize these problems but provide indirect observations of the structures. Indeed, some of the finest images of lamellar morphology have been obtained through electron microscopy of surface replicas. However, atomic force microscopy (AFM) is a nondestructive scanning microscopic technique which allows direct observation of the original surface, yielding local *three-dimensional* information in real space. Direct imaging of bulk or film surfaces, or microtomed sections thereof, either in air or in liquid, has been used to study the morphology of both crystalline<sup>14,34</sup> and liquid crystalline polymers.<sup>35</sup> In most cases, AFM alleviates the need to extract the subject from its original matrix, thus allowing *in situ* polymer studies.<sup>36</sup> High-resolution AFM has become a valuable tool in the resolution of molecular structure<sup>37</sup> and, in the case of i-PP, the direct observation of helix sense in a crystal has been reported.<sup>13</sup>

Table 1. Polymer Physical Properties

polymer	$T_m$ (K)	$T_g$ (K)	$M_w^a$	$M_w/M_n$
PRECH, PSECH	$411 \pm 1$	$247 \pm 1$	450 000	1.6
50/50 blend	$411 \pm 1$	$247 \pm 1$		

<sup>a</sup> Approximate values as determined by GPC analysis against polystyrene standards.

In this paper we report the results of a detailed investigation of the morphology, using AFM, of melt-crystallized spherulites of optically pure poly(*R*-epichlorohydrin) (PRECH) and poly(*S*-epichlorohydrin) (PSECH) and the equimolar blend of the polyenantiomers. The aim of this work is to determine the effects of backbone macromolecular chirality on the lamellar assembly within melt-crystallized, banded spherulites. We demonstrate that the effects of the asymmetric centers are expressed beyond the level of the lamellae to the gross morphological level of the spherulite. The present study is unique in reporting the direct observation, by AFM, of spherulite spiral sense in isochiral, banded spherulites. The images presented herein substantiate the interpretation of our previous results.<sup>21</sup>

### Experimental Section

The synthesis and the characterization of the isotactic optically active poly(*S*-epichlorohydrin), poly(*R*-epichlorohydrin), and the preparation of their equimolar blend have been described elsewhere.<sup>21</sup> Some physical properties of the polymers are included in Table 1. The samples were prepared for AFM by first pressing the polymer between two silicon wafers (Semiconductor Processing Inc., Boston, MA) on a hotplate at 175 °C until the polymer melted. The silicon wafer assembly was transferred to a thermally controlled (Linkam TMS91) microscope hotstage (Linkam THMS600) at 175 °C, where the polymer was melted for 15 min under a nitrogen atmosphere and then cooled at a rate of 130 °C/min to a crystallization temperature of 70 °C, where it was held isothermally for 30 min. The silicon wafer assembly was then removed from the hotstage and immersed in liquid nitrogen. This treatment permitted the top silicon wafer to be removed easily, leaving a polymer film of the desired thickness, *ca.* 30–50  $\mu$ m. The remaining bottom wafer and polymer film were then reinserted into the hotstage and melted at 175 °C for 15 min, cooled at a rate of 130 °C/min to a constant crystallization temperature and allowed to crystallize unrestrained for 4 h under a nitrogen atmosphere.

The AFM images were recorded in air using an AutoProbe CP scanning probe microscope (Park Scientific Instruments, Sunnyvale, CA) operating in either the constant-force mode or constant-height mode, as indicated, using a 100  $\mu$ m scanner operating at a scanning frequency of 2.0 Hz. The cantilevers employed were Microlevers and Sharp Microlevers (Park Scientific) which had a nominal radius of 500 and 200 Å, respectively, and a spring constant of 0.05 N/m. Where indicated, AFM images scanned with a constant force were subjected to a high-pass filter.

Polarized light optical micrographs were taken with a Nikon 35 mm camera mounted onto a Nikon Optiphot polarized light optical microscope. Reflectance light micrographs were taken with an Olympus 35 mm camera mounted onto a Leitz reflectance microscope. The radial line intensity profile of the polarized light optical micrograph in Figure 2c was obtained using JAVA video analysis software (Jandel Scientific).

### Results and Discussion

As we have shown previously, upon isothermal crystallization from the melt over a wide range of temperatures, the optically pure enantiomers of poly(epichlorohydrin) form spherulites that exhibit a banded morphology when viewed optically by transmitted polarized light.<sup>21</sup> As Figure 1a demonstrates, the banding pattern of the isochiral spherulites is also evident upon microscopic viewing of the free surface by reflected light.

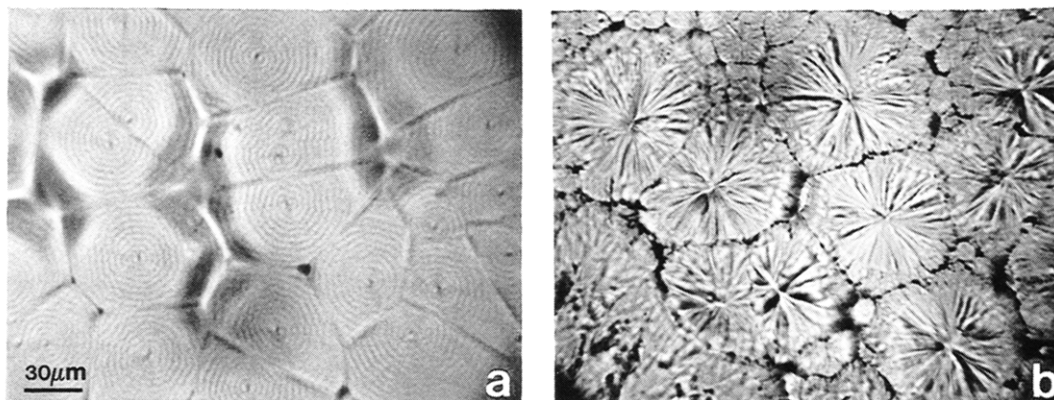


**Figure 1.** Reflectance optical micrographs of the unrestrained melt-crystallized spherulitic film crystallized at 80 °C of (a) the optically pure PSECH and (b) the equimolar blend.

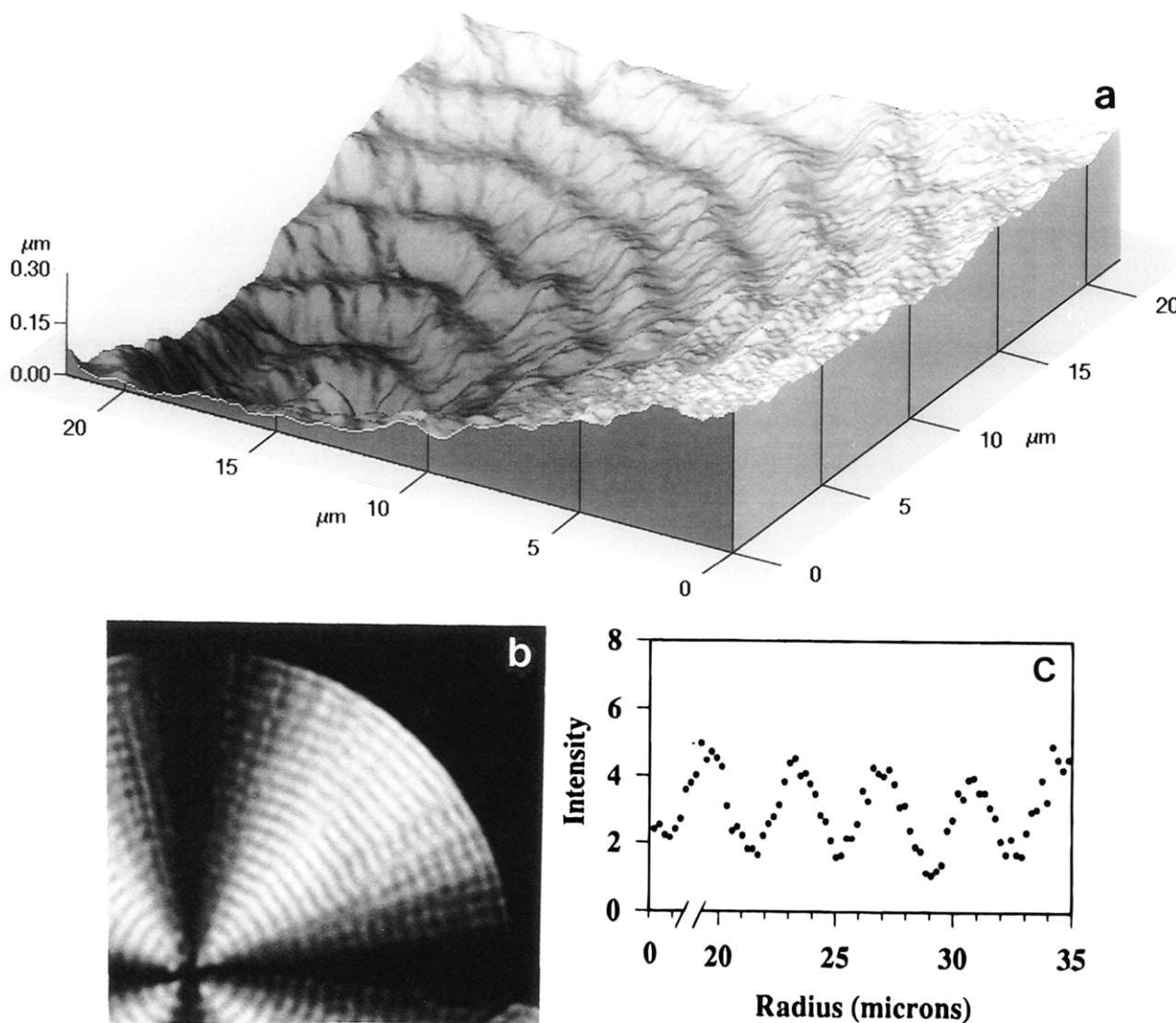


**Figure 2.** (a) Three-dimensional AFM image of a quadrant of an optically pure PSECH spherulite surface crystallized unrestrained at 80 °C, scanned in the constant-force mode; (b) the corresponding polarized light optical micrograph; and (c) the radial line intensity profile, showing the band periodicity of the banded spherulite section in (b).

This morphology is in sharp contrast to the nonbanded spherulites which form from the melt of the equimolar blend of the enantiomers, under identical crystallization conditions. The reflectance light micrograph in Figure 1b shows the relatively coarse surface texture of the unbanded spherulites.

The unrestrained melt-crystallized polymer films of the optically active polyenantomers typically contain

spherulites in which the nucleus is situated in a central pit. This feature is demonstrated clearly in the three-dimensional AFM image of a quadrant of the optically pure poly(*S*-epichlorohydrin) spherulite surface shown in Figure 2a. This image was generated while scanning the surface of the spherulite in the constant-force mode, with the dark regions indicating depth. These pitlike depressions are of the order of 20  $\mu\text{m}$  in diameter and

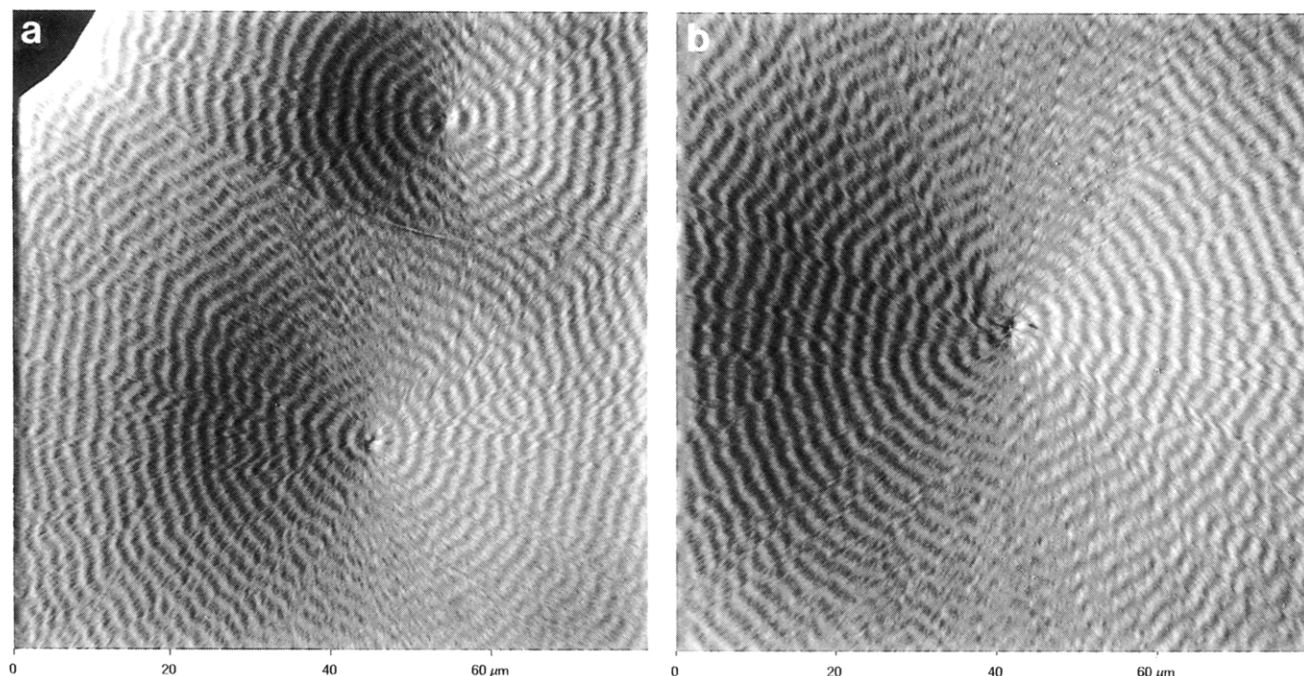


**Figure 3.** Low-magnification AFM image scanned in constant-height mode of (a) an optically pure PSECH spherulite and (b) an optically pure PRECH spherulite, both melt-crystallized unrestrained at 75 °C.

are typically of the order of 1  $\mu\text{m}$  deep. This feature is not uncommon to spherulites grown with a free top surface<sup>10,22,26,38a</sup> and presumably reflects the exhaustion of crystallizable material which prevents symmetry in three dimensions. Certainly these depressions are much more open than the central holes reported by Lustiger et al.<sup>10</sup> for polyethylene spherulites grown in much thicker films. The periodic topographical pattern of ridges and valleys, clearly visible in Figure 2a, is characteristic of the spherulite surface of the optically pure enantiomers of poly(epichlorohydrin). In a previous study of banded spherulites of poly(trimethylene glutarate), Keller<sup>22</sup> noted that in vertical illumination the bands of the spherulites were visible as steps or ledges on the surface of the unrestrained spherulites. The AFM image in Figure 2a, which is similar in appearance to the spherulite fragment of poly(trimethylene glutarate) shown in Figure 7 of ref 22, demonstrates physically the presence of such ledges along the incline of the pitlike depression in the banded spherulite of PSECH. The corresponding polarized light optical micrograph of poly(*S*-epichlorohydrin) is shown in Figure 2b with its sectional analysis showing the band spacing in Figure 2c. The periodicity of the birefringent extinction banding pattern corresponds directly to the periodicity of the surface contour banding of the spherulite as measured by AFM.

Figures 3a and b contain the raw, low-magnification AFM images of the free spherulitic surfaces of the *S*- and *R*-polyenantiomers, respectively, obtained while scanning in the constant-height mode. The coherence of the surface bands is striking. The bright bands in the AFM image indicate elevated regions, measured to lie approximately 400 Å above the dark band regions at the highest point. The elevated bands are regions in which the lamellae are oriented edge-on. These bands correspond to the birefringent (bright) bands under the polarized light microscope. The alternating surface crests and troughs of the unrestrained banded spherulites as imaged by AFM confirm an alternating flat-to-edge-on lamellar orientation, inferred from simi-

lar electron micrographs of surface replicas of similarly banded spherulitic surfaces of polyethylene<sup>2</sup> and poly(vinylidene fluoride).<sup>26</sup>

Figures 4a and b contain the corresponding raw AFM images of the area surrounding the nucleus of the *S*- and *R*-polyenantiomer spherulites, respectively, collected while scanning the free surfaces in a constant-force mode. The filtered images of Figures 4a and b are shown in Figures 4d and e, respectively. Upon close inspection of these images, it is apparent that the lamellae, in their edge-on orientation, maintain a unique sense of inclination throughout the spherulite. A comparison of Figures 4c and d leads to the observation that these edge-on lamellae are inclined in opposite directions for the two polyenantiomers. The prominent feature of the AFM images of the isochiral spherulites is the overall appearance of a spiral, originating at the nucleus and continuing with a *unique* sense of direction throughout the surface of the spherulite, although it becomes somewhat less coherent toward the edges of the larger spherulites. More striking is the observation that the sense, or handedness, of the spiral is uniquely related to the chirality of the constituent polyenantiomer. When viewed looking down onto the free surface, the AFM images of the banded PSECH spherulite surfaces consistently display a counterclockwise spiral sense, while those of the PRECH spherulite surfaces exclusively manifest the opposite, clockwise spiral sense. The sense, or handedness, of a spherulite formed from the optically pure polyenantiomer with a characteristic nucleus pit can be determined readily upon inspection of the surface by AFM. Only in rare cases was the spiral not immediately apparent. With a common viewing perspective, the handedness of the spiral is always opposite for spherulites of polyenantiomers of opposite chirality.

In contrast to the present case, previous studies with nonoptically active polymers have reported that the two directions of spiral twist are observed to occur with equal probability in the banded spherulites which display surface spiral morphologies.<sup>22,38b</sup> The sense of the spiral was always maintained within one spherulite



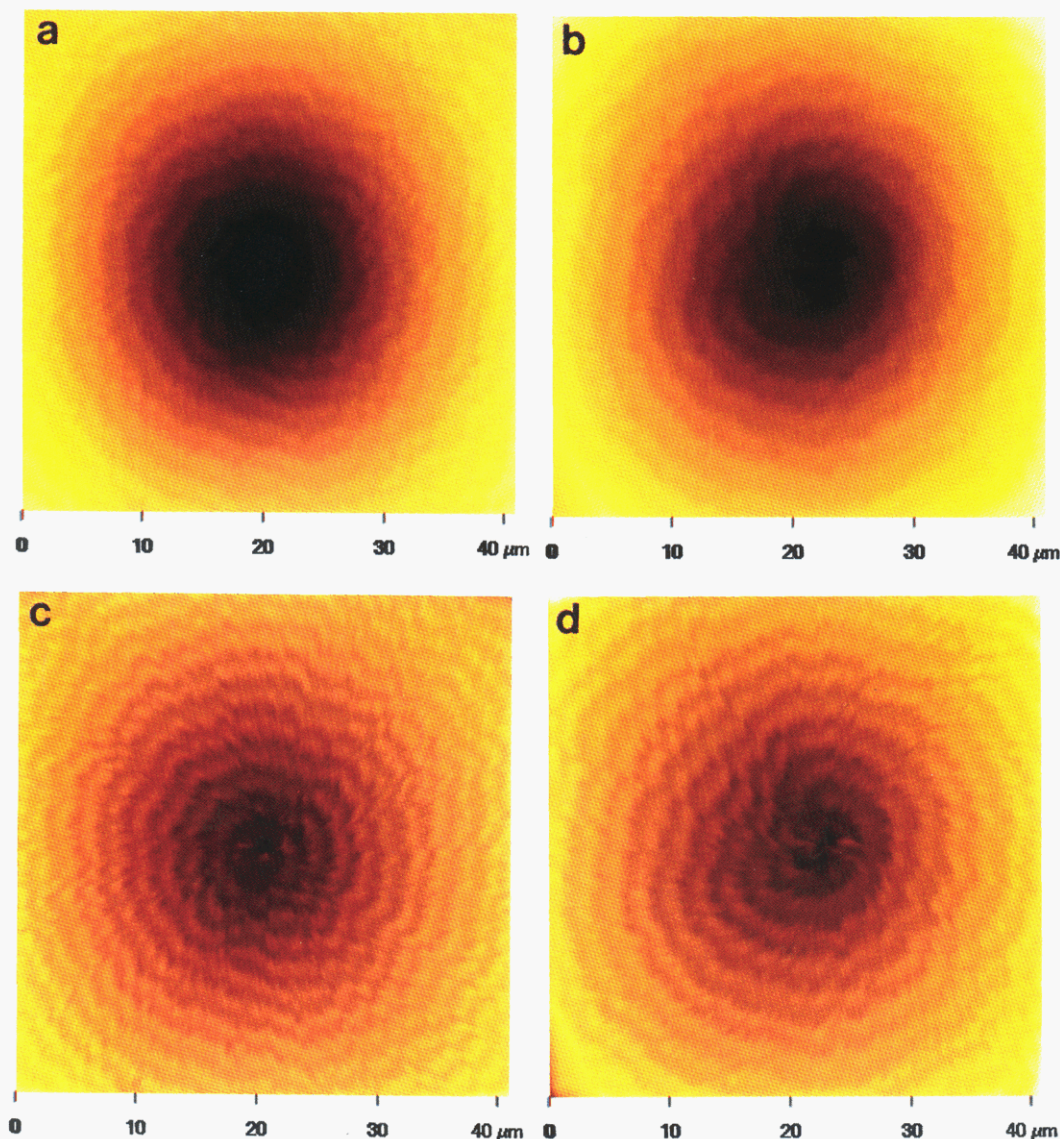


**Figure 4.** Higher magnification AFM images of the corresponding spherulites in Figure 3 scanned in constant-force mode of (a) PSECH and (b) PRECH; (c) the high-pass-filtered image of (a); (d) the high-pass-filtered image of (b). Note the unique direction of inclination of the lamellar edges in each of the isochiral spherulite surface images.

or at least within an undisturbed sector. Apart from early work by Keller,<sup>22</sup> who first noted that the bands of the poly(tetramethylene glutarate) spherulites were effectively spirals, these observations in polymer systems have principally been made for polyethylene.<sup>23–24,38a,39a,b</sup> In those previous investigations of the free surfaces, by reflected light and electron microscopy of the surface replicas, the sense of the spiral was accented due to the inclination of the apparently edge-on oriented lamellae in the direction of the spiral. The same inclination phenomenon is manifested in the isochiral spherulites in this study.

In those previous studies, it was suggested that the sense of a regularly twisted lamella is developed early in the formation of the spherulite and maintained throughout the growth.<sup>38c</sup> Mathematical models developed to account for surface spiral morphology in polyethylene were based on the assumption that the twisted lamellae interdependently form part of a continuous, predictable structure throughout the banded spherulite.<sup>40</sup> The mathematical models arranged the twisting lamellae in a radial fashion such that the locus of all points of a given lamellar twist within the spherulite generated a continuous surface of a three-dimensional

spiral form. In more recent work by Lustiger et al.,<sup>10</sup> the experimentally observed surface morphology of banded polyethylene spherulites was also accurately represented by a computer-modeled surface projection of an assembly of radially oriented same-sense twisted lamellae. Graphical representations of oblique sections which dissect radially growing helicoids predicted different lamellar surface projections of the model spherulite. Depending on the angle of the dissection plane to the lamellae and the position of the plane on the helicoidal axis, the resulting lamellar profiles projected onto that plane varied from straight-line to S- and C-shaped lamellar geometries, all of which can be seen experimentally for polyethylene. Only the C-shaped lamellar profiles permitted the ready determination of the direction of the coordinate twist of the lamellae, or the handedness of the helicoid. It was both predicted and found experimentally that C-shaped lamellae would project onto the spherulitic surface when the nucleus was about 5–15 helicoidal periods below. In our current study of the highly organized optically active poly-(epichlorohydrin) system, the determination of the sense of the isochiral spherulite spiral was most easily ascertained when the nucleus was observed to be at the

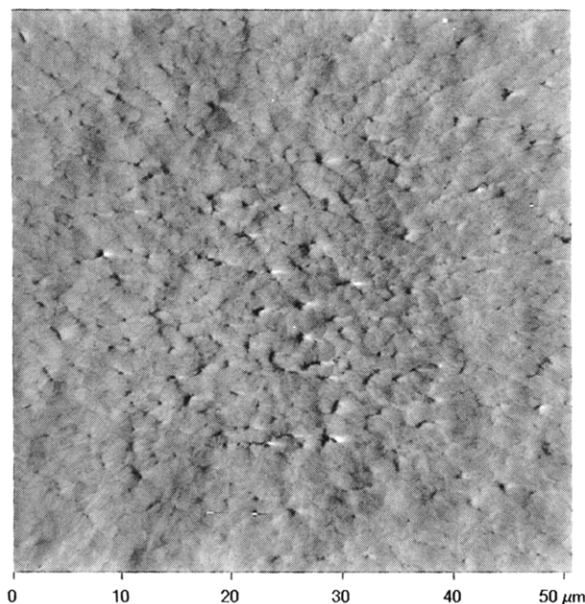


**Figure 5.** AFM image of the unrestrained melt-crystallized surface of the equimolar blend spherulite crystallized at 80 °C scanned in constant-height mode.

bottom of a pitlike depression with a radius of about five band periods.

The phenomenal effect on the spherulitic morphology that results from the mixing of the two polyenantionomers to form an equimolar blend is demonstrated in the AFM image shown in Figure 5. Clearly, the level of cooperativity that is required for long-range coherence of the lamellae, in both the radial growth direction and circumferentially, which exists in the isochiral spherulites, is absent in the spherulites formed from the equimolar blend. The black marks on the AFM image of the blend spherulite indicate deep holes and cracks between some neighboring groups of lamellae.

The AFM images of a higher magnification afford a more detailed look at the lamellar organization in spherulites of the PSECH polyenantionomer (Figure 6a) and of the equimolar blend (Figure 6b). The radial growth direction is from left to right in each image with the nucleus out of view. In (a) it is difficult to follow a particular lamella, or group of lamellae, through a series of flat and edge-on orientations because the growth direction of the radiating lamellae does not remain parallel to the viewing surface over as many bands.<sup>24</sup> In (b) short-range order is visible in the equimolar blend sample as many small bunches of flat, somewhat coherent lamellae. The size of a typical bunch is of the order of 1  $\mu\text{m}^2$ .

Due to sample flow during the melting period, the film thickness is reduced considerably at the edges. Consequently, in these regions the supply of crystallizable material is exhausted early and results in immaturely formed spherulites and dendritic structures. Although these structures are crystallized under the same thermal conditions as the spherulites in the melt-rich sections of the film, the former crystallize at a slower rate due to the lack of crystallizable material. The images of these regions of the optically pure PSECH and the equimolar blend are shown in the reflected light micrographs in Figures 7a and b, respectively. In the PSECH sample, these dendritic structures have a counterclockwise pinwheel-like appearance, reflecting the counterclockwise twisting sense of the mature spherulite counterpart shown earlier. These curved

dendritic structures closely resemble those of polyethylene grown under similar conditions for which it was reported that the pronounced same-sense curvature of the flat-on lamellae reflects the tendency toward same-sense twisting in thicker, banded spherulites, not restricted by film thickness.<sup>41</sup> In (b) the straight branches of the equimolar blend structures are visible. The surfaces of these dendritic structures are depicted in the corresponding low-magnification AFM images in Figures 8a and b. Higher magnification AFM images of the apparent branch points in the dendritic structures for the optically pure PSECH and the equimolar blend samples are presented in Figures 8c and d, respectively. Collectively, the lamellae are turning on edge at the branch point in the optically pure PSECH polyenantionomer structure. However, in the equimolar blend structure the branches appear to be composed of layers of flat lamellae, each layer measured to have a thickness of the order of 100 Å.

The dendritic structures in Figures 7 and 8 are similar in appearance to the crystal aggregates of the banded,  $\alpha$ -phase of poly(vinylidene fluoride) (PVF<sub>2</sub>), grown from very dilute melts of a binary blend with a noncrystallizable polymer as observed by Briber and Khoury.<sup>42</sup> The structures displayed radially twisting lamellae that periodically fanned out with a period which corresponded to that of the banded spherulites formed from the melt under the same thermal conditions. The twisting phenomenon was attributed to unequal fold surfaces due to staggered chain folds, as described by Keith and Padden for polyethylene,<sup>9</sup> while the splaying feature was attributed to a periodic release of stress buildup between stacks of lamellae. Without mention of twist sense, it was suggested that the combined twisting–splaying motif is the underlying structure in banded spherulites, as opposed to simply helicoidal twisting. Although the structures formed from a viscous, amorphous heterogeneous melt and the present dendritic structures formed in thin sections of a homogeneous melt have apparently similar morphologies, we consider the splaying in the poly(epichlorohydrin) structures to be indicative of an insufficient supply of crystallizable material.

**On Lamellar Twisting.** Ordered arrays of identical geometrical units give rise to a regular, repeated pattern upon observation at a larger level. The overall shape of the isochiral lamellae reflects the molecular geometry of the closely packed, same-sense helices from which they are constituted. The ordered arrays of these densely packed, isochiral lamellae consequently impart a characteristic surface appearance to the spherulites formed from the optically active macromolecule. Consider a slice of an isochiral lamella dissecting the radial growth direction at right angles, so that it contains essentially a monolayer of chain stems of isochiral helices. Such an arrangement can be considered as a two-dimensional array of long chiral rods of a given handedness. This arrangement can also be defined by an idealized plane (containing the length of the rods) of the nematic phase of a liquid crystal. It has been shown for liquid crystalline polymers that when the rods are all isochiral, the free energy is lowered when neighboring *planes* align the long axis of their respective isochiral rods slightly less than parallel.<sup>43–44</sup> The effect of the backbone chirality of the chains in a *chiral* nematic phase is thus to generate the resultant *cholesteric* phase in which the direction of molecular chain stem orientation rotates in a periodic, helical fashion. By analogy



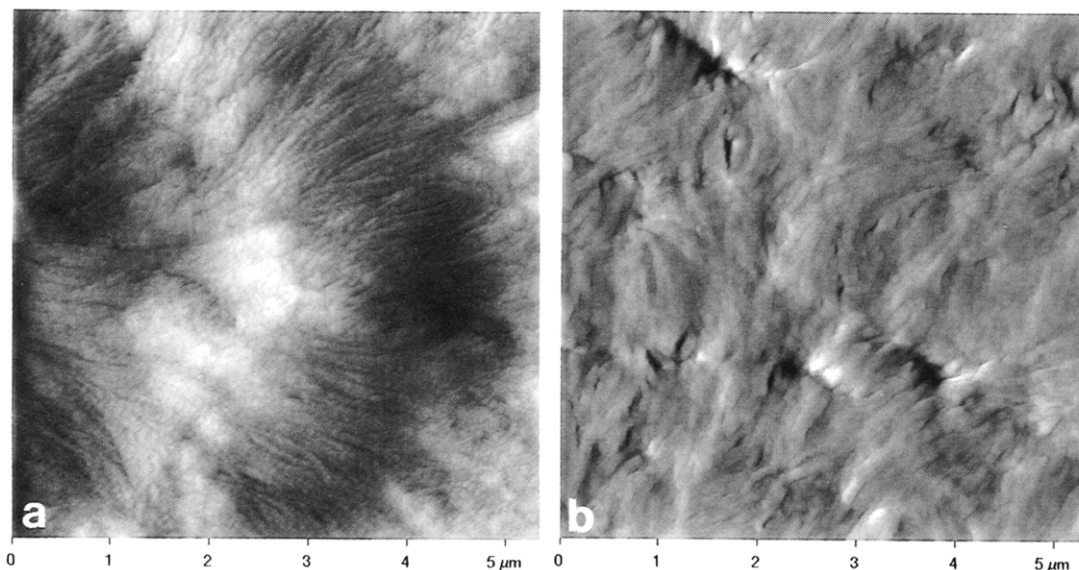


**Figure 6.** High-magnification AFM images of the unrestrained surface of the melt-crystallized spherulite at 80 °C scanned in constant-height mode of (a) the optically pure PSECH and (b) the equimolar blend.

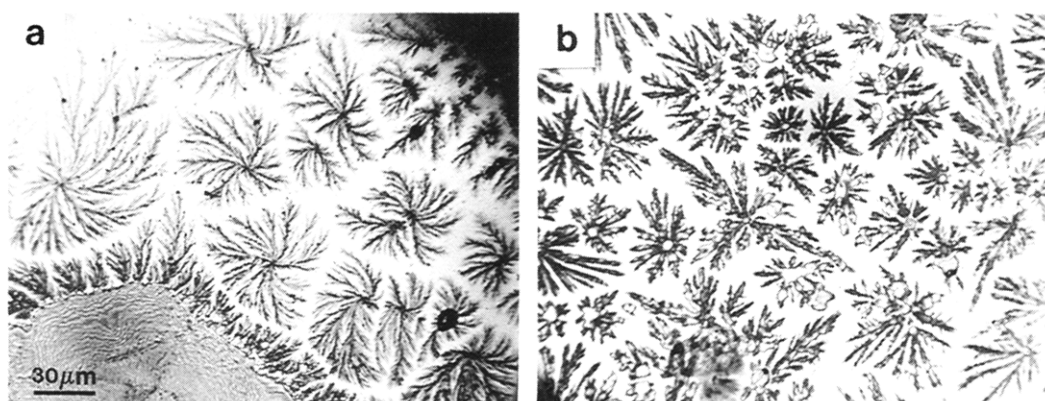


**Figure 7.** Reflectance optical micrographs of the melt-crystallized dendritic structures grown in thin sections of the film at 80 °C of (a) the optically pure PSECH and (b) the equimolar blend.

to cholesteric liquid crystalline polymers, it is conceivable then that regularly twisted, helicoidal isochiral lamellae could result from the effect of the lowering of the lateral free energies of the constituent chain-folded isochiral helices. In this way, the two possible twist directions of a lamella composed exclusively of chiral helices of one handedness are expected to be energetically nondegenerate. What emerges is a *true* chiral factor which determines the direction of lamellar twist. It is attributed to the handedness of the constituent molecular helices, which in turn is determined by the macromolecular backbone chirality. Indeed, the inclination of the concerted lamellae in the low-magnification AFM images of the spherulitic surfaces depends directly on the chiral nature of the polyenantiomers comprising the isochiral spherulite. Similarly, the observation of the unique spherulitic spiral sense, dependent upon the chirality of the constituent polyenantiomer, is in keeping with the transmission of the effects of the molecular geometry to the higher order structures.

The observed dependence of spherulite morphology on backbone chirality has not been reported previously for melt-crystallized synthetic polymers. However, it can be related to a similar observation by Lotz et al.<sup>45</sup> in a study of chain-folded single crystals and crystal aggregates of silk fibroin and its model enantiomer polypeptides from solution. The direction of the lamel-

lar twist was constant along the length of the lamella and was observed to be dictated by the chirality of the asymmetric amino acid residues in the chains; i.e., there was an intralamellar origin to the lamellar geometry. Although the pitch of the lamellar twist in the polypeptide crystal structures is comparable to the bandwidth in banded spherulites, the polypeptides do not have a similar bandwidth dependence on crystallization temperature. Indeed, in this previous work by Lotz et al., the successive rotation of the neighboring chain stems was compared specifically to the rotation of the chain axes in the cholesteric liquid crystalline form of poly( $\gamma$ -benzyl glutamate).<sup>43</sup> They maintained that the intralamellar origin of the geometry involved the core of the lamella. They noted that although the presence of surface stresses from nonorthogonal chain stems cannot be ruled out as a contributing factor to the twist, it cannot entirely account for the lamellar geometry.

In general, the chain stems in a lamella can maintain a nonorthogonal relationship to the opposite fold surfaces either by canting toward the radius of the spherulite or in a tangential direction. Keith and Padden<sup>9</sup> have predicted that the surface stresses which result from the former will cause the formation of predominantly *helically* twisted lamellae. There are reports of banded polyester spherulites in which the chains are known to be inclined toward the radius.<sup>46</sup> For chain canting in the tangential direction, they predict the

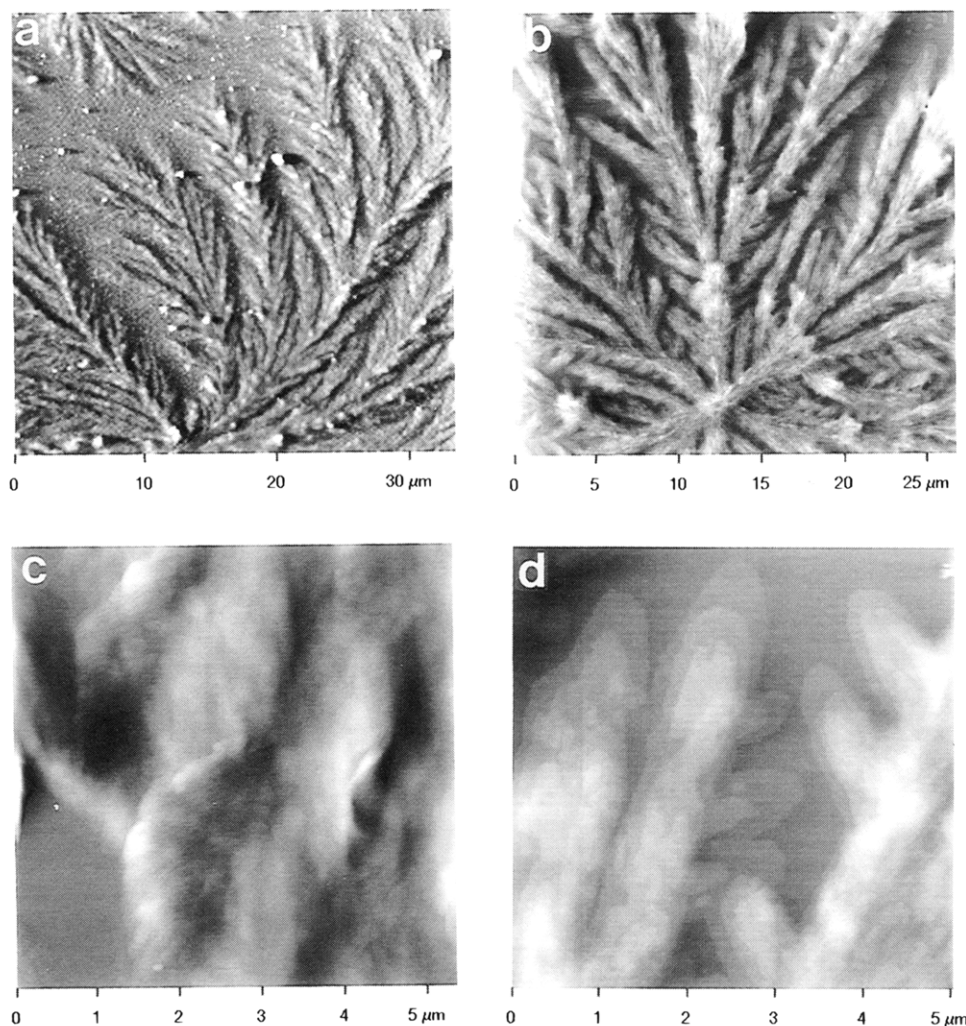


**Figure 8.** Low-magnification AFM images of the dendritic structures depicted in Figure 7 of (a) the optically pure PSECH, (b) the equimolar blend, and (c and d) their respective higher magnification AFM images. (All of the images were collected using constant-height mode.)

formation of *helicoidally* twisted lamellae, as in the case of banded polyethylene spherulites. Although the chain stems are successively rotated in the tangential direction in the cholesteric liquid crystal phase analogy, this does not require that the chains be tilted with respect to the lamellar normal. It is not known whether or not the chains are canted in poly(epichlorohydrin). However, it should be noted that the *c* axes of regularly rotating chain stems in helicoidally twisted lamellae can still maintain an orthogonal relationship with the lamellar fold surfaces.<sup>45b</sup>

Surely, beyond the confines of the planar zigzag polyethylene system there are lamellar twist-determining factors other than chain canting. In his studies of PVF<sub>2</sub>, Vaughan<sup>26</sup> found that although the chains in the  $\gamma$ -phase spherulites are known to be tilted with respect to the lamellar normal, the lamellae have a curved but untwisted profile and banding is not observed. It was not known whether chain canting occurs in the  $\alpha$ -phase, which forms banded spherulites with predominantly planar lamellae demonstrating an alternating flat-on to edge-on orientation along the *b*-axis growth direction in the spherulite surface replicas. Lovinger et al.<sup>47</sup> have demonstrated that in the  $\alpha$ -phase of PVF<sub>2</sub> the dipolar chains are statistically packed so that there is a cancellation of the dipole vectors of the unit cell while in the  $\gamma$ -phase the lamellae are composed of polar unit cells. Thus, macromolecular backbone polarity can affect the

way chains arrange in the unit cell and consequently influences the organization of unit cells in the lamellae. These effects are manifested in the gross morphology as banded spherulites.

The extinction of any long-range cooperativity of the lamellae in the spherulites in an equimolar blend of the two polyenantiomers lends support to a stereoselection at the growth front in the blend spherulites, as we have suggested earlier.<sup>21</sup> However, the extent to which chains of the opposite-sense polyenantiomer are excluded from the lamellae remains unresolved. The exclusion of opposite-sense helices in the equimolar blend may be incomplete. The condensation of some adjacent enantiomeric chains at the growth front would interrupt a regular lamellar twist and, in some instances, represent points of helicoidal twist reversal. Indeed, Cothia<sup>48</sup> suggested that the presence of achiral residues in twisted  $\beta$  sheets of polypeptides should decrease the tendency of the lamellae to twist, perhaps even canceling the effect. The lamellae may well be turning on their edge in the blend spherulite, albeit randomly and without any significant interlamellar long-range order, giving rise to a coarse, incoherent birefringent pattern and collectively, a relatively flat spherulitic surface. It is well known that the coarse, fibrillar appearance of nonbanded spherulites arises from the edges of the lamellae as they intersect the surface.<sup>49</sup>



In view of the large number of crystalline species that form banded spherulites,<sup>50</sup> which extends far beyond polymeric materials, it appears that an explanation of such a widespread phenomenon involves the very general prerequisite of a necessary level of *asymmetry*. Such a general prerequisite can account for the common banded spherulitic features among small molecules and chain-folded structures while still recognizing the inherent differences among these crystalline species. Apparently, the element of asymmetry is not essential at the level of the residue, specifically. For example, in polyethylene, asymmetry is introduced only at the level of the tertiary structures, i.e., the compression anisotropy at the opposite lamellar fold surfaces induced by the chain tilting within one lamella. As for the more complex PVF<sub>2</sub> system,<sup>26</sup> the presence of more than one element of asymmetry may be influencing the lamellar organization, namely, those of macromolecular polarity and chain canting. The PVF<sub>2</sub> case may also indicate the importance of the strength of the asymmetric element. Ultimately, not every asymmetric element will have such pronounced effects on the crystallization process.

### Summary and Conclusions

In the highly organized poly(epichlorohydrin) system the backbone chirality of the polymer chains imposes significant restrictions on the lamellar organization within the spherulites of both of the enantiomers and their equimolar blend. The observed differences in the spherulitic surface morphologies among the polyenantiomers and their equimolar blend support our initial suggestion that a stereoselective mechanism occurs at the growth front in the blend spherulite. The significant loss of coordination among the lamellae in the equimolar blend in both the radial and circumferential directions of the unrestrained spherulitic surface supports this claim. In contrast to the long-range in-phasing of the lamellae in the polyenantiomer spherulites, the equimolar blend spherulites manifest only patches of local, short-range order. Bunches of lamellae collectively give a relatively flat surface. Often neighboring bunches are not in close contact but are separated by gaps in the surface of the order of 1000 Å deep. However, the extent of the exclusion of oppositely handed helices from the lamellae in the equimolar blend system is not resolved. An incomplete stereoselection mechanism at the growth front of the equimolar blend spherulites is suggested, where the periodic incorporation of opposite-sense chains present locations of regular lamellar twist interruption and/or helicoidal twist reversal.

The observed surface morphology of the banded, isochiral spherulites of PSECH and PRECH is consistent with previously modeled surfaces of a spherulitic architecture composed of an assemblage of radiating helicoidally twisted lamellae.<sup>10</sup> No evidence was seen to indicate that regularly spaced screw dislocations along the lamellae accommodate the twisted molecular orientation in the banded spherulites, as described in the model developed by Bassett.<sup>6</sup> The observed morphology favors the existence of an underlying lamellar geometry of radiating, regularly twisted helicoidal lamellae, as in the model by Keith and Padden.<sup>9</sup> The nature of the intralamellar origin of such a geometry, however, appears to depend on the molecular characteristics of the poly(epichlorohydrin). It is not known whether the chains are tilted with respect to the lamellar normal in optically active poly(epichlorohy-

drin). However, for these polyenantiomers it would seem that the factor which determines the direction of twist of the lamellae is the chiral identity of the chains. Although stresses at the opposite fold surfaces cannot be excluded, it is suggested that the twist of the lamellae arises from the lowering of the lateral surface free energies of the isochiral helices as they condense in slightly less than parallel *layers* in the lamellar growth direction. Indeed, the molecular geometry of the isochiral helices is translated beyond the lamellar level to that of the spherulite, the surface of which manifests a spiral, the direction being dependent upon the handedness of the constituent polyenantiomer. For optically active poly(epichlorohydrin) the asymmetrical units present in the backbone of the optically pure polyenantiomer are actively influencing the development of the overall spherulite and their effects are transmitted to the level of the gross morphology.

**Acknowledgment.** Financial support in the form of operating grants from the Natural Science and Engineering Research Council, Canada, and Fonds FCAR, Quebec, is gratefully acknowledged. The authors wish to express their appreciation to A. Badia, Department of Chemistry, McGill University, for assistance in recording the AFM images and to Dr. R. St. John Manley for helpful discussions and suggestions.

### References and Notes

- (1) Keller, A. J. *Polym. Sci.* **1955**, 17, 351.
- (2) Fischer, E. W. *Z. Naturforsch.* **1957**, 12A, 753.
- (3) Price, F. P. *J. Polym. Sci.* **1959**, 39, 139.
- (4) Fujiwara, Y. *J. Appl. Polym. Sci.* **1960**, 4, 10.
- (5) Keller, A.; Sawada, S. *Makromol. Chem.* **1964**, 74, 190.
- (6) Bassett, D. C.; Hodge, A. M. *Polymer* **1978**, 19, 469.
- (7) Bassett, D. C.; Hodge, A. M. *Proc. R. Soc. London* **1981**, A377, 25.
- (8) Bassett, D. C.; Olley, R. H.; Al Raheil, A. M. *Polymer* **1988**, 29, 1539.
- (9) Keith, H. D.; Padden, F. J., Jr. *Polymer* **1984**, 25, 28.
- (10) Lustiger, A.; Lotz, B.; Duff, T. S. *J. Polym. Sci., Polym. Phys. Ed.* **1989**, 27, 561.
- (11) Toda, A.; Keller, A. *Colloid Polym. Sci.* **1993**, 271, 328.
- (12) Bassett, D. C.; Freedman, A. M. *Prog. Colloid Polym. Sci.* **1993**, 92, 23.
- (13) Snetivy, D.; Vansco, G. J. *Polymer* **1994**, 35, 461.
- (14) Lotz, B.; Wittman, J. C.; Stocker, W.; Magonov, S. N.; Cantow, H.-J. *Polym. Bull.* **1991**, 26, 209.
- (15) Snetivy, D.; Guillet, J. E.; Vansco, G. J. *Polymer* **1993**, 34, 429.
- (16) Lotz, B. *Philos. Trans. R. Soc. London A* **1994**, 348, 19.
- (17) Bruckner, S.; Meille, S. V.; Petraccone, V.; Pirozzi, B. *Prog. Polym. Sci.* **1991**, 16, 361.
- (18) Lotz, B.; Wittmann, J. C. *J. Polym. Sci., Polym. Phys. Ed.* **1986**, 24, 1541.
- (19) Stocker, W.; Magonov, S. N.; Cantow, H.-J.; Wittmann, J. C.; Lotz, B. *Macromolecules* **1993**, 26, 5915.
- (20) Li-Sheng, L.; Stupp, S. I. *Macromolecules* **1995**, 28, 2618.
- (21) Singfield, K. L.; Brown, G. R. *Macromolecules* **1995**, 28, 1290.
- (22) Keller, A. *J. Polym. Sci.* **1959**, 39, 151.
- (23) Keith, H. D.; Padden, F. J., Jr. *J. Polym. Sci.* **1959**, 39, 101.
- (24) Keith, H. D.; Padden, F. J., Jr. *J. Polym. Sci.* **1959**, 39, 123.
- (25) Patel, D.; Bassett, D. C. *Proc. R. Soc. London A* **1994**, 445, 577.
- (26) Vaughan, A. S. *J. Mater. Sci.* **1993**, 28, 1805.
- (27) Schultz, J. M.; Kinloch, D. R. *Polymer* **1969**, 10, 271.
- (28) Bassett, D. C.; Vaughan, A. S. *Polymer* **1985**, 26, 717.
- (29) Keller, A. *J. Polym. Sci.* **1955**, 17, 291.
- (30) Hoffman, J. D.; Lauritzen, J. I. *J. Res. Natl. Bur. Stand.* **1961**, 65A, 297.
- (31) (a) Olley, R. H.; Hodge, A. M.; Bassett, D. C. *J. Polym. Sci., Polym. Phys. Ed.* **1979**, 17, 627. (b) Bu, H. S.; Cheng, S. Z. D.; Wunderlich, B. *Polymer* **1988**, 29, 1603. (c) Palmer, R. P.; Cobbold, A. *Makromol. Chem.* **1964**, 74, 174. (d) Priest, D. J. *Polym. Sci., Part A-2* **1971**, 9, 1777.

- (32) Wittman, J. C.; Lotz, B. *J. Polym. Sci., Polym. Phys. Ed.* **1985**, *23*, 205.
- (33) Kanig, G. *Kolloid Z.* **1973**, *251*, 782.
- (34) See ref 13 and other papers in this series.
- (35) (a) Fischer, H.; Miles, M. J.; Odell, J. A. *Macromol. Rapid Commun.* **1994**, *15*, 815. (b) Patnaik, S. S.; Bunning, T. J.; Adams, W. W.; Wang, J.; Labes, M. M. *Macromolecules* **1995**, *28*, 393.
- (36) See, for example: Shakesheff, K. M.; Davies, M. C.; Roberts, C. J.; Tendler, S. J. B.; Shard, A. G.; Domb, A. *Langmuir* **1994**, *10*, 4417.
- (37) Dietz, P.; Hansma, P. K.; Ihn, K. J.; Motamedi, F.; Smith, P. *J. Mater. Sci.* **1993**, *28*, 1372.
- (38) (a) Geil, P. H. In *Polymer Single Crystals*; Mark, H. F., Immergut, E. H., Eds.; John Wiley & Sons: New York, 1963; p 230. (b) See p 247 in (a). (c) See p 248 in (a).
- (39) (a) Keller, A. In *Growth and Perfection of Crystals*; Doremus, R. H., Roberts, B. J., Turnbull, D., Eds.; Wiley: New York, 1958; p 499. (b) Geil, P. H. *J. Polym. Sci.* **1961**, *51*, 510.
- (40) Thornton, A. W.; Predecki, P. *J. Appl. Phys.* **1970**, *41*, 4266.
- (41) Keith, H. D.; Padden, F. J., Jr.; Lotz, B.; Wittman, J. C. *Macromolecules* **1989**, *22*, 2230.
- (42) Briber, R. M.; Khoury, F. *J. Polym. Sci., Polym. Phys. Ed.* **1993**, *31*, 1253.
- (43) Robinson, C. *Tetrahedron* **1961**, *13*, 219.
- (44) Grosberg, A. Y. *Sov. Phys. Dokl.* **1980**, *25*, 638.
- (45) (a) Lotz, B.; Gonthier-Vassal, A.; Brack, A.; Magoshi, J. *J. Mol. Biol.* **1982**, *156*, 345. (b) See Figure 6 in (a).
- (46) Keith, H. D. *Macromolecules* **1982**, *15*, 114, 122.
- (47) Lovinger, A. J.; Amundson, K. R. *Polym. Prepr. (Am. Chem. Soc., Div. Polym. Chem.)* **1993**, *31*, 784.
- (48) Cothia, C. J. *J. Mol. Biol.* **1973**, *75*, 295.
- (49) Claver, G. C., Jr.; Buchdahl, R.; Miller, R. L. *J. Polym. Sci.* **1956**, *20*, 202.
- (50) (a) Ryschenkow, G.; Faivre, G. *J. Cryst. Growth* **1988**, *87*, 221. (b) Bisault, J.; Ryschenkow, G.; Faivre, G. *J. Cryst. Growth* **1991**, *110*, 889. (c) Lagasse, R. R. *J. Cryst. Growth* **1994**, *140*, 370. (d) See ref 38, this paper.

MA950758G